

Search for PeV-EeV Tau Neutrinos and Optical Transients from Violent Objects with Ashra-1

Y. AITA¹, T. AOKI¹, Y. ASAOKA¹, H.M. MOTZ¹, M. SASAKI¹, C. ABIKO², C. KANOKOHATA², S. OGAWA², H. SHIBUYA², T. TAKADA², T. KIMURA³, J. G. LEARNED⁴, S. MATSUNO⁴, S. KUZE⁵, P. M. BINDER⁶, J. GOLDMAN⁶, N. SUGIYAMA⁷, AND Y. WATANABE⁸ (ASHRA-1 COLLABORATION)

¹ *Institute for Cosmic Ray Research, University of Tokyo, Kashiwa, Chiba 277-8582, Japan*

² *Department of Physics, Toho University, Funabashi, Chiba 274-8510, Japan*

³ *College of Engineering, Ibaraki University, Hitachi, Ibaraki 316-8511, Japan*

⁴ *Department of Physics and Astronomy, University of Hawaii at Manoa, Honolulu, HI 96822, USA*

⁵ *Center for Environmental Remote Sensing, Chiba University, Chiba 263-0022, Japan*

⁶ *Department of Physics and Astronomy, University of Hawaii at Hilo, Hilo, HI 96720-4091, USA*

⁷ *Department of Physics and Astrophysics, Nagoya University, Nagoya, Aichi 464-8601, Japan*

⁸ *Department of Engineering, Kanagawa University, Yokohama, Kanagawa 221-8686, Japan*

sasakim@icrr.u-tokyo.ac.jp

Abstract: Ashra is a project to build an unconventional optical telescope complex that images a very wide field of view (FOV), covering 77% of the sky, yet with the angle resolution of a few arcmin, with the use of image intensifier and CMOS technology. The project primarily aims to observe Cherenkov and fluorescence light from air-shower developments. It can also be used to monitor optical transients in the wide FOV. The detector has great sensitivity in the PeV-EeV region using the Earth-skimming (ES) tau neutrino technique, and can be used to search for neutrinos originating from hadron acceleration in astronomical objects. Additional advantages are perfect shielding of cosmic ray secondaries, precision determination of arrival direction, and negligible atmospheric neutrino background. Ashra-1 completes its 3rd observation period, the first dedicated to taking physics data for PeV-EeV tau neutrinos with the best instantaneous sensitivity and optical transients, in March 2013. From January 2012 until end of March 2013, about 1950 hours of data have been taken out of 2006 hours possible due to light constraints. For optical transients, we have 3763 additional hours of data taken from 2008 until 2011. We present the analysis of these data taken for the PeV-EeV tau neutrinos and optical transients.

Keywords: gamma-ray burst, tau neutrino, optical flash, air-shower, transient

1 Introduction

Gamma-ray bursts (GRBs) eject the most energetic outflows in the observed universe, with jets of material expanding relativistically into the surrounding interstellar matter with a Lorentz factor Γ of 100 or more. Energy dissipation processes involving nonthermal interactions between particles are thought to play an important role in GRBs. The GRB standard model [1], which is based on internal/external shock acceleration, has been used to describe the general features of a GRB, but the jet structure and particle acceleration details remain observationally unresolved. In the context of the GRB standard model, the interaction of an expanding relativistic shell with the interstellar medium (ISM) involves two shocks: the forward shock, which explains observed multi-wavelength afterglow, and the reverse shock, which is predicted to produce a strong optical flash [2, 3]. The explanation of optical flashes by the reverse shock has led to some estimates of the initial Lorentz factor η [3, 4]. The presence of accelerated protons at the GRB site must be a reality. The detection of PeV-EeV neutrinos (ν s) from a GRB provides direct evidence for the acceleration of hadrons into the EeV range, and of photo-pion interactions in the GRB. Even the non-detection of neutrino can provide valuable information about GRB's key physical parameters such as the emission radius R_d , and the bulk Lorentz factor Γ [5].

2 Ashra Experiment and Observation

Ashra-1 uses electrostatic lenses [9] in addition to an optical system to generate convergent beams, enabling a very low cost and high performance image sensor, providing a high resolution over a wide FOV. The electron optics use an image pipeline to transport the image from the focal sphere of the reflective mirror optical system. After the light from the image is split, it is transported to both a trigger device and high-gain, high-resolution complementary metal-oxide semiconductor (CMOS) image sensor. The image pipeline technique enables very fine images with parallel self-triggers independently with same optical system for optical flash, air-shower Cherenkov light in operation, and fluorescence light under commissioning in 2013.

The all-sky survey high-resolution air-shower detector (Ashra) is a complex of unconventional optical collectors that image VHE air showers in a 42° diameter field of view (FOV) covering 77% of the entire night sky with a resolution of a few arcminutes [6, 7, 8]. The first phase of the Ashra experiment (Ashra-1) was constructed on Mauna Loa at 3300 m above sea level on Hawaii Island, and includes an observatory.

Ashra-1 acquires optical images every 1~6 s with short readout deadtime. This enables us to explore optical transients, possibly associated with violent objects such as GRBs in so far as they are brighter than $B = 12 \sim 13$ mag, for which we expect 3σ signals assuming 4 s exposure.

Satellite	GRB Name	$t_{inFOV} - t_0$ [sec]
Swift	GRB081203A	$-1.2 \times 10^4 - 5.6 \times 10^3$
Fermi	GRB090428	$-8.1 \times 10^3 - 5.9 \times 10^3$
Fermi	GRB090429C	$-4.1 \times 10^3 - 1.7 \times 10^3$
Swift	GRB091024	$-1.6 \times 10^3 - 3.3 \times 10^2$
Fermi	GRB100216A	$-4.0 \times 10^3 - 1.1 \times 10^4$
Swift	GRB100906A	$-1.0 \times 10^4 - 4.0 \times 10^3$
Fermi	GRB120120	$-1.4 \times 10^3 - 8.9 \times 10^3$
Fermi	GRB120129	$-1.6 \times 10^3 - 6.7 \times 10^3$
Fermi	GRB120327	$-9.9 \times 10^3 - 8.2 \times 10^1$
Swift	GRB120911	$-2.4 \times 10^4 - 6.8 \times 10^1$
Fermi	GRB121019	$-1.7 \times 10^3 - 7.3 \times 10^3$
Swift	GRB121212A	$-5.8 \times 10^3 - 2.6 \times 10^4$
Fermi	GRB130206	$-3.3 \times 10^3 - 7.5 \times 10^4$
Fermi	GRB130215	$-2.7 \times 10^3 - 4.3 \times 10^2$

Table 1: Summary of coincidence events with satellite GRB triggers [13, 14]. List of gold-plated events which must be observable geometrically within the FOV of our light collector at satellite triggers during our observation time.

The unique advantage is the on-time detection of the events without resorting to usual satellite alerts. In each detector unit FOV, 1~2 events per year are expected in coincidence with the Swift gamma-ray events. The total Ashra field of view that is wider than satellite instruments allows to detect more optical transients, including an interesting possibility for an optical flash, not visible with gamma-rays.

The earth-skimming tau neutrino (ν_τ) technique, which detects extensive air showers [10], has the advantage of a large target mass, since it uses air showers produced by decay particles of tau leptons (τ s) in the atmosphere as the observed signals. τ s emerge out of the side of the mountain or the ground facing the detector; they are the product of interactions between VHE ν_τ and the earth matter they traverse. Above 1 EeV, air fluorescence observations based on the earth-skimming ν_τ technique have been reported [11]. Ashra-1 has reported the first observational search for ν_τ from a GRB based on the earth-skimming ν_τ technique with air showers induced by τ decays (hereafter referred to as the Cherenkov τ shower method) [12]. It can achieve sufficient detection sensitivity in the PeV–EeV region to be useful in the search for ν s originating from hadrons accelerated to EeV at astronomical objects. Additional advantages of the Cherenkov τ shower method are its perfect shielding of cosmic-ray secondary particles, highly precise arrival direction determination for primary ν_τ and negligible background contamination by atmospheric ν s in the PeV–EeV energy range.

Two of the Ashra-1 light collectors has been used for optical flash observation, of which FOV centers are in the direction of 60° (0° N) and 12° (22.5° N) in the elevation (azimuthal) angles respectively. We recorded more than 3 million non-trigger recurring images of the FOV of 0.83 sr for 5637 hr of 1121 night runs between June 28 in 2008 and March 23 in 2013. The observation time corresponds to 20 % of all time without the shutdown period for the maintenance and 95 % of the maximum observable time defined by the solar and the lunar conditions where the altitudes of the sun and the moon must be lower than -18° and 0° respectively with the moon fraction less than 0.2.

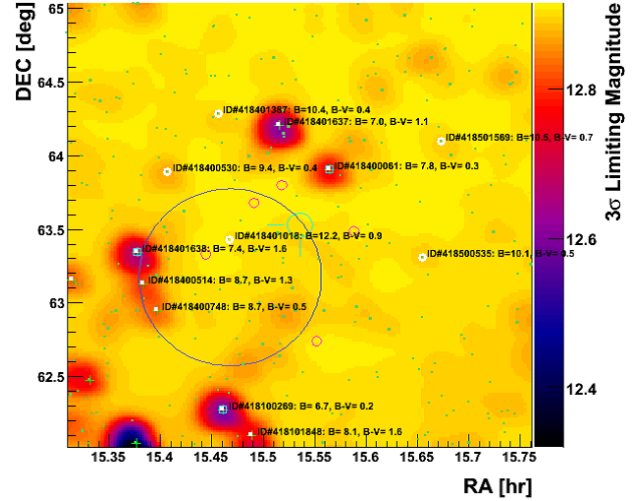


Figure 1: 3σ limiting map for prompt optical flash GRB081203A.

To investigate GRB optical emission, we define three specific observational time domains with respect to satellite triggers; precursor ($0 < t_0 - t_e < 24$ hr), prompt ($t_s < t_0 < t_e$), and afterglow ($0 < t_s - t_0 < 3$ hr) where t_0 is a satellite trigger time, t_s is the time when the trajectory of the center position of GRB counter part object triggered by the satellite enters into a FOV of an Ashra-1 light collector and t_e is the time when it exits the FOV. Throughout the above observation time for optical flashes and afterglows, we preselected and categorized 32 (86), 6 (21), and 1 (4) GRBs triggers by Swift (Fermi) satellite, which were circulated through The Gamma-ray Coordinates Network (GCN) [13, 14], into the three time domains respectively as optical transient candidates. Furthermore, we selected gold-plated samples of 14 prompt GRB candidate events for our cross observation with Swift or Fermi satellites requiring the events triggered are reported as trigger type of GRB as summarized in Table 1.

One of the Ashra light collectors built on Mauna Loa has the geometrical advantages of not only facing Mauna Kea, allowing it to encompass the large target mass of Mauna Kea in the observational FOV, but has also an appropriate distance of ~ 30 km from Mauna Kea, yielding good observational efficiency when imaging air-shower Cherenkov lights which are directional with respect to the air-shower axis. Using the advanced features, we performed commissioning search for Cherenkov τ showers for 197.1 hr between October and December of 2008 and have already published [12]. We served limited 62 channels of photomultiplier tubes (PMTs) as trigger sensors prepared for the commissioning runs to cover the view of the surface area of Mauna Kea, maximizing the trigger efficiency for Cherenkov τ showers from Monte Carlo (MC) study. Adjacent-two logic was adopted to trigger the fine imaging, by judging discriminated waveform signals from each pixel of the multi-PMT trigger sensor. During the commissioning search period, ~ 2 hr before the trigger of GRB081203A [15]. We accumulated nearly 44 million images with the air-shower Cherenkov light triggers for 1863 hr of 323 night runs of the ν_τ search between January 12 in 2012 and March 23 in 2013.

3 Analysis

Our wide field observation covered the Swift-BAT error circle at the time of GRB081203A [15]. We have searched for optical emission in the field of GRB081203A around the BAT-triggered GRB time (T_0) with one of the light collector units in the Ashra-1 detector. The Ashra-1 light collector unit used in this analysis has the achieved resolution of a few arcmin, viewing 42° circle region of which center is located at $Alt = 11.7^\circ$, $Azi = 22.1^\circ$. The sensitive region of wavelength is similar with the B-band. We quickly analyzed 83 images covering the field of GRB081203A every 7.2s with 6s exposure time respectively during the observation between T_0-300s and T_0+300s . We detected no new optical object within the PSF resolution around the GRB081203A determined by Swift-UVOT. As a result of our preliminary analysis, the 3σ limiting magnitudes were estimated in comparison with stars in Tycho-2 Catalog to be distributed between 11.7 and 12.0 for time bins corresponding to 4 s exposure time.

Our observation also covered the Swift-BAT error circle at the time of GRB100906A [16]. We searched for optical emission in the field of GRB100906A around T_0 with an Ashra-1 light collector, viewing 42° circle region of which center is located at $Alt = 60^\circ$, $Azi = 0^\circ$. We analyzed 200 images covering the field of GRB100906A every 6s with 4s exposure time respectively during the observation between T_0-600s and T_0+600s . We detected no new optical object within the PSF resolution around the GRB100906A determined by Swift-UVOT. In the same manner as GRB081203A, the 3σ limiting magnitudes were estimated and they were distributed between 12.0 and 12.2 for individual time bins corresponding to 4 s exposure time. All original RAW format images of the preselected event samples were converted into Fits format files. A set of dark image frames were prepared for every night runs at the Mauna Loa observation site. Another set of image frames for the procedure of gain flat were made for every observational season, which is defined as a period between full moon ages, using uniformly illuminating spherical plate scintillator with the same curvature radius of the input focal sphere of our photoelectric lens imaging tube (PLI). The calibration procedure was performed at the beginning and the ending of each observational season with the spherical plate scintillator put on the input window of PLI. The quantitative quality of the gain calibration can be checked using the night sky background images taken as flat images with the same Ashra-1 light collector, followed by a procedure of the median flat method. The gain calibration error was confirmed to be less than several % with the comparison between the gain calibration with scintillation and checks with the median flat procedure.

Once image data are prepared after the dark and gain flat procedures, we perform two kinds of main data processes of astrometry and photometry as conventional astronomical procedure. Contrary to the astronomical convention we use so wide angle photoelectrical optics that we needed to consider gradually converging procedure of matching observed sources with catalog stars. First of all we extracted observed sources from each image using the SExtractor program [20] and compared with the positions and B and V filter brightness of stars preselected from the Tycho2 Catalog [21] to be within FOV of the light collector. The matching procedure started with the brightest stars to be in FOV and gradually compared with fainter ones until all observed sources should be matched with the pres-

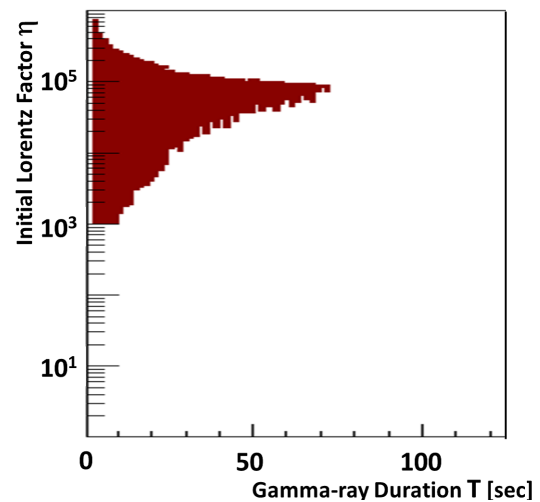


Figure 2: Constrain of the 3σ rejection area (dark) for the initial Lorentz factor as varying the GRB duration.

ected catalog stars. We have checked this scheme using 572 test pairs of real observed sources and tycho2 catalog stars and confirmed that the estimated source positions and magnitudes are fairly consistent with the catalog ones with negligible failures in matching. The matching error on the position is confirmed to be less than 1 CMOS pixel corresponding to the resolution of 1.4 arcmin in the Ashra-1 optical system. In the final stage of the astrometry, we determined the position of the GRB counter part at the satellite trigger time as well as the local coordinate system using at least 3 reference stars as close to the GRB position as possible in the observed image.

For the procedure of the photometry, again we used near observed stars as references, of which B and V magnitudes are well known to estimate the detection sensitivity of the Ashra-1 light collector. Adding that we checked the fluctuation of the background of each image using the output ADC values of CMOS pixels in the region not containing effectively bright stars after applying Gaussian filter with the measured point spread to images to eliminate photon statistical fluctuation. The estimated signal to noise ratio (SNR) in the background region was confirmed to be consistent Gaussian distribution with the standard deviation of unity without any tailed events. Finally we made the SNR map and the map of 3σ limiting magnitude for each selected image.

For physics interpretation, we deal with the parameter of real gamma-ray duration as a free parameter taking into account the threshold effect of the satellite triggers. Following the assumption of the duration, we needed to change the time bin width to estimate the limiting magnitude of the detection sensitivity. Figure. 1 shows the map of 3σ limiting magnitude as a preliminary result of the search of prompt optical flash from GRB081203A.

The unique check of optical flash around the GRB satellite trigger time can lead to the estimates of the initial value of the Lorentz factor η with another assumed parameter of gamma-ray duration time T following the procedure described in [22] and combining with the other multi-wavelength observations of the afterglow from GRB081203A [23]. Figure. 2 shows the preliminary result of the constrain of the initial Lorentz factor as varying the

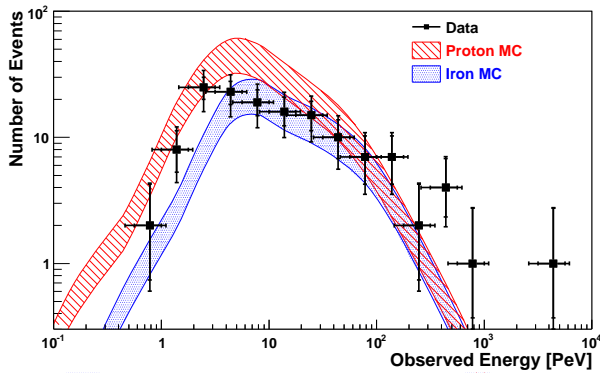


Figure 3: Observed cosmic-ray flux spectrum (filled box) with bars indicating statistical and systematic errors and the MC predictions for proton primary (hatched band) and iron primary (shaded band) assumptions [17]. The width of the bands shows the evaluated systematic error of 30% of the MC prediction.

parameter of gamma-ray duration from the search for optical flash from GRB081203A.

The estimation of the detection sensitivity, background, and pointing accuracy of the Ashra light collector as an ES ν_τ detector and the validity of the reconstruction procedure are described elsewhere [24]. To confirm the detection sensitivity and gain calibration for the Cherenkov τ shower, we detected and analyzed 140 events of normal cosmic-ray air-shower Cherenkov images for a total of 44.4 hr in 2008 December and 1863 hr between July 11 in 2011 and March 23 in 2013, using the same instruments used in neutrino observation, but after rearranging the trigger pixel layout to view the sky field above Mauna Kea. In the cosmic-ray observation, the trigger pixel layout is centered at zenith angle of $\sim 65^\circ$. The observed and MC cosmic-ray flux spectra are shown in Fig. 3, in which the MC prediction used the typically observed cosmic-ray flux in the knee region [18, 19]. Since the primary cosmic-ray components are observationally undefined, we present the MC prediction of cosmic-ray flux spectra, assuming either only protons or irons as the primary cosmic rays in Fig. 3. Note that the same reconstruction procedure was applied to both of the observed and MC data to extract the observed energy. In both cases, the observed data and the MC prediction agreed well on the normalization and the shape of the distribution within the expected errors.

4 Discussions

Non-detection of optical flash classifying time domains of violent burst such as GRBd provides valuable information about GRB's key physical parameters such as the initial Lorentz factor η . The great point source sensitivity for ν_τ is shown in Fig. 4. Assuming unknown point sources with the total ν_τ fluence of $8.72 \text{ GeV cm}^{-2} \text{ E}^{-2}$ which corresponds to diffuse flux of $3.6 \times 10^{-8} \text{ GeV sr}^{-1} \text{ cm}^{-2} \text{ s}^{-1}$ to causes the cosmic neutrino candidate events IceCube reported from 670.1 days of livetime [25], the currently operational Ashra-1 detects can detect 77 and 49 signal τ events with the directional accuracy within 0.1° and no physics background. The narrow skimming angle, which limits the coincidence rate of detecting τ point sources with one light

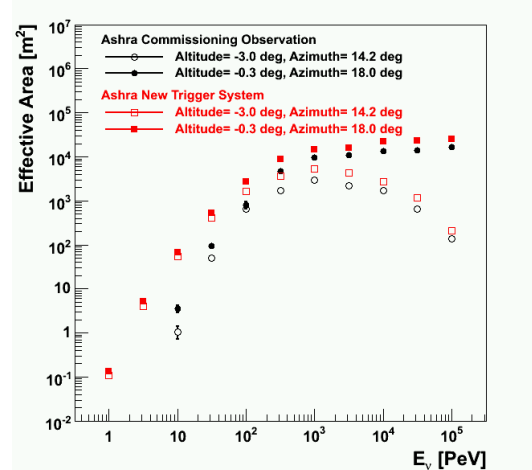


Figure 4: Effective area of Cherenkov τ shower ES method with Ashra-1 for the Obs03 period in 2012-2013 (square) and for the past commissioning phase (circle) in 2008, in the cases of (altitude, azimuth) of $(-0.3^\circ, 14.2^\circ)$ (filled) and $(-3.0^\circ, 18.0^\circ)$ (opened) respectively.

collector in Ashra-1, will be dramatically improved in the Ashra NTA project with multi-station large arrays to detect large angle up-coming regenerating τ s using fluorescence as well as Cherenkov air-shower light [26]. Ashra-1 plans to start another commissioning operation of fluorescence trigger readout adding to the optical flash and the Cherenkov τ ES and CR ones in November 2013..

References

- [1] Mészáros, P. 2006, Rep. Prog. Phys., 69, 2259
- [2] Mészáros, P., & Rees, M.J. 1997, ApJ, 476, 232
- [3] Sari, R., & Piran, T., 1999. ApJ, 517, L109
- [4] Mészáros, P., & Rees, M.J. 1999, MNRAS, 306, L39
- [5] Gao, S., *et al.* 2013, arXiv:1305.6055
- [6] Sasaki, M. 2008, J. Phys. Soc. Japan, 77SB, 83
- [7] Aita, Y., *et al.* 2008a, Proc. 30th ICRC, 3, 1405
- [8] Sasaki, M., *et al.* 2008, Proc. 30th ICRC, 3, 1559
- [9] Asaoka, Y., & Sasaki, M. 2011, Nucl. Instr. and Meth. A, 647, 34
- [10] Fargion, D. 2002, ApJ, 570, 909
- [11] Abraham, J., *et al.* 2008, Phys. Rev. Lett., 100, 211101
- [12] Aita, Y., *et al.* 2011, ApJL, 736, L12
- [13] http://gcn.gsfc.nasa.gov/swift_grbs.html
- [14] http://gcn.gsfc.nasa.gov/fermi_grbs.html
- [15] Y. Aita *et al.*, GCN Circ., 8632 (2008).
- [16] Y. Asaoka *et al.*, GCN Circ., 11291 (2010).
- [17] Y. Aita *et al.*, ApJL736, L12 (2011).
- [18] Antoni, T., *et al.* 2005, Astropart. Phys., 24, 1
- [19] Amenomori, M., *et al.* 2008, ApJ, 678, 1165
- [20] Bertin, E. and Arnouts, S. 1996, A&AS, 117, 393
- [21] Høg, E., *et al.*, 2000, A&A, 355, L27
- [22] Kobayashi, S. and Zhang, B., 2003, ApJ, 582, 641
- [23] <http://gcn.gsfc.nasa.gov/other/081203A.gcn3>
- [24] Asaoka, Y. and Sasaki, M., 2013, , 41, 7
- [25] Ishihara, A., 2012, , Proc. Suppl. 00, 1-6
- [26] Aita, Y., *et al.* 2013, Proc. 33rd ICRC, Cont.#1030